18PB-4

Improved Laser-to-Proton Conversion Efficiency in Isolated Reduced Mass Targets.

A. Morace[1,2], C. Bellei[2], T. Bartal[3],L. Willingale[4], J, Kim[3], A. Maksimchuk[4], K. Krushelnick[4], M. S. Wei[5], P. K. Patel[2], D. Batani[6], N. Piovella[7], R. B. Stephens[5] and F. N. Beg[3]
[1] Institute of Laser Engineering, Osaka University, 2-6 Yamadaoka, Suita, Osaka, Japan.
[2] Lawrence Livermore National Laboratory, 7000 East Avenue, Livermore, CA 94550, U.S.
[3] Center for Energy Research, University of California, 9500 Gilman Drive, La Jolla, CA 92093, U. S.
[4] University of Michigan, 2200 Bonisteel Blvd. Ann Arbor, MI 48109, U. S.
[5] General Atomics, 3550 General Atomics Court, San Diego, CA 92121, U. S.
[6] CELIA, Université de Bordeaux-1, 351, Cours de la Libération F-33405 Talence, France.
[7] Dipartimento di Fisica, University of Milano, via Celoria 16, 20133 Milano, Italy.

We present experimental results of laser-to-proton conversion efficiency as a function of lateral confinement of the refluxing electrons. We demonstrate that the laser-to-proton conversion efficiency increases by 50% with increased confinement of the target from surroundings with respect to a flat target of the same thickness. Three-dimensional hybrid particle-in-cell simulations using LSP code agree with the experimental data. The adopted target design is suitable for high repetition rate operation as well as for Inertial Confinement Fusion (ICF) applications.

1. Introduction

In the laser-driven ion acceleration scheme termed target-normal-sheath-acceleration (TNSA) [1], the relativistic electrons produced set up a space-charge electric field at the target rear surface as they exit. Such field immediately ionizes the hydrocarbon molecules (present on the surface as impurities) and accelerates the ions, especially protons due to their higher charge-to-mass ratio.

However, the quality of the proton beam still needs to be improved under several aspects. The one discussed in this work is improving the energy conversion efficiency from lasers to protons [2,3]. In this work we study the relation between target isolation and laser-to-proton energy conversion efficiency, using a set of RMTs of the same size, and varying their isolation from the large support foil by decreasing the size of the linking legs.

2. Experimental setup

The experiment was performed using the T-Cubed laser at the Center for Ultrafast Optical Science (CUOS), University of Michigan, Ann Arbor. The Nd:glass laser, with central wavelength at 1053 nm, delivered 5 J of laser energy in 400 fs and was tightly focused onto the target front surface with 20 mm focal spot size resulting in a average intensity of 3×10^{18} W/cm^2. As shown in Fig. 1, laser-machined RMT (150 μm square,10 μm thick) were only attached to a 10 mm thick surrounding Cu foil by means of 4 legs having variable size (21, 42 and 84 μm) for each target and a constant 106 μm length. Smaller leg size corresponds to a higher RMT isolation. In addition, large (3mm x 3mm) uniform, 10 μm thick Cu foil targets were also used as comparison.

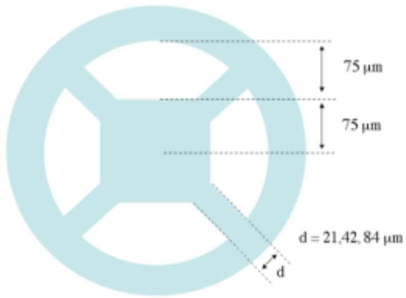

Fig. 1. Schematic of the laser-cut RMT targets.

A stack of Radio-chromic film (RCF), Gafchromic HD-810 [4] was used as a proton beam diagnostic. The RCF stack was positioned 4 cm from the target rear surface and was protected with 12.5 μm Al foil, allowing protons with energies equal or higher than 1.05 MeV to deposit energy in the first RCF foil active.

3. Experimental results and simulation.

The RCF images were digitized with a calibrated scanner and the total dose was then evaluated in krads. The dose deposited on the first and second layers corresponds to proton energies above 1.05 MeV, and 3.1 MeV respectively (see Fig. 2).

In order to understand the effect of target isolation on proton conversion efficiency and spectra, 3D hybrid particle-in-cell (PIC) simulations using the LSP code [5] have been performed. The RMT is represented by a 75 μm radius disk connected to the supporting foil by 4 legs with size of 21 and 84 μm respectively. In addition, the completely isolated RMT and a simple large Cu foil are also modeled. A fully ionized H contaminant layer (2 μm thick) is included on both the front and the rear target surfaces, including the connecting legs and the supporting Cu foil.

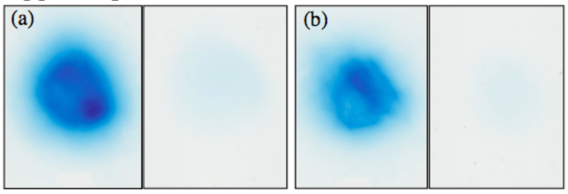

Fig. 2. Collected RCF data for (a) 21 mm leg width and (b) 84 mm leg width.

An exponential fast electron distribution is injected, with slope temperature of 1.1 MeV in 400 fs full-width half maximum Gaussian temporal profile, resulting in a total injected energy of 1.46 J.

In Fig. 3, the *quantitative* comparison between experiment and simulations is shown. We assumed a laser-to-fast-electron conversion efficiency of 30% to calculate the simulated, energy-normalized deposited dose. This is consistent with experimentally inferred values [6].

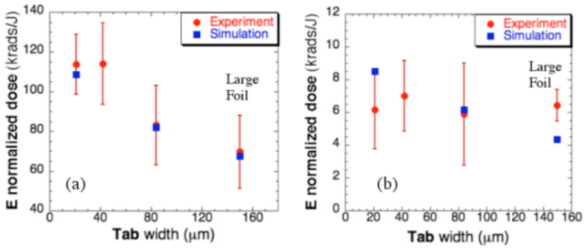

Fig. 3. Experimental and simulated energy normalized integrated dose as function of the RMT leg size for first RCF (a) and second RCF layer (b).

For the first RCF, sensitive to proton energies above 1.05 MeV, with larger contribution by protons in the 1-2 MeV range (due to the Bragg curve), the comparison between the trend of simulated normalized dose vs. leg width and that of the experimental data are in excellent agreement. Although the rather large error bars and the laser-to-fast electron energy conversion efficiency assumption do not allow to claim a perfect quantitative agreement, the 3D axis-cylindrical simulations accurately describe the physics in our experimental conditions. The dose deposited in the second RCF was an order of magnitude smaller than in the first one. This feature is captured by the simulations too (Fig. 3b).

Figure 4 shows the time integrated proton kinetic energy as a function of time; it demonstrates how the laser-to-proton conversion efficiency is highly dependent on the target isolation.

We observe that even though the initial acceleration stage is similar for all targets corresponding to the protons with maximum kinetic energy, at around 1.4 ps (or 0.4 ps after the end of the injection) the curves start to separate. The acceleration saturates earlier for poorly isolated targets; conversely, the higher the isolation, the longer is the acceleration of the protons and hence the higher is the laser-to-proton conversion efficiency.

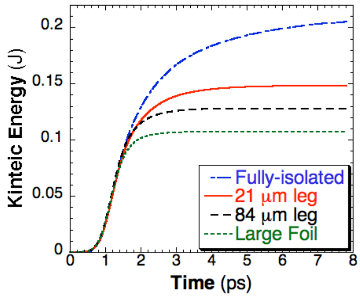

Fig. 6. Proton (forward accelerated) total kinetic energy vs. time, for the four types of targets. The proton acceleration is initially identical and starts diversifying at about 1.4 ps simulation time, or 0.4 ps after the injection.

Finally, from the simulation data it is possible to estimate the laser-to proton conversion efficiency. Considering only the forward-accelerated protons with energy above 1.05 MeV, the calculated laser-to-proton conversion efficiencies at 6 ps simulation time (when the total proton kinetic energy is fully saturated) are 3, 2.5 and 2.1 % for the 21mm leg, 84 mm leg and large foil cases, corresponding to an efficiency increment of about 50 % for highly isolated targets, with respect to large foils.

4. Conclusion

In summary, in this paper we have demonstrated in both experiments and 3D PIC simulations that the use the use of thin legs has been reduces the loss rate of fast electrons escaping from the acceleration foil due to the radial spread and results in a significant increase of the proton acceleration time. We observe that the smaller the leg size (i.e., the higher the isolation with respect to the supporting structure), the higher is the conversion efficiency.

References

[1] S. C. Wilks et al. Phys. Plasmas 8, 542 (2001).
[2] S. Buffechoux et al. Phys. Rev. Lett 105, 015055 (2010).
[3] O. Tresca et al. PPCF 53, 105008 (2011).
[4] D. S. Hey et al. Rev. Sci. Inst. 79, 053501 (2008).
[5] D.R. Welch et al. Comp. Phys. Comm. 164 (2004) 183–188.
[6] M. H. Key et al. Phys. Plasmas **5**, 1966 (1998).